



Cite this: *Chem. Commun.*, 2025, 61, 11441

Received 12th May 2025,  
Accepted 18th June 2025

DOI: 10.1039/d5cc02692j

rsc.li/chemcomm

## Improved light harvesting *via* energy transfer within a benzothiadiazole-based antenna–sensitizer dyad for dye-sensitized solar cells<sup>†</sup>

Rossella Infantino, <sup>a</sup> Elena Ermini, <sup>ab</sup> Carmen Coppola, <sup>acd</sup> Irene Motta, <sup>ef</sup> Gregorio Bottaro, <sup>ef</sup> Lidia Armelao, <sup>eg</sup> Adalgisa Sinicropi, <sup>acd</sup> Alessandro Mordini, <sup>ab</sup> Gianna Reginato, <sup>a</sup> Massimo Calamante, <sup>ab</sup> Lorenzo Zani, <sup>a</sup> Daniele Franchi <sup>\*a</sup> and Alessio Dessi <sup>\*a</sup>

We describe the design, synthesis and application in dye-sensitized solar cells (DSSCs) of a fully organic dyad consisting of a visible light-harvesting D–A–π–A dye covalently linked to a small antenna that can absorb higher energy photons. Thanks to its precise molecular design, not previously applied in DSSCs, the dyad showed an excellent overlap between the antenna emission spectrum and the dye absorption spectrum, providing a high energy transfer efficiency of 88%, which is among the best reported for such systems. Cells featuring the dyad as a sensitizer showed increased light-harvesting efficiency compared to those built with a reference dye without the antenna, resulting in a 35% higher average power conversion efficiency.

Improving light harvesting efficiency (LHE) in the visible and near-IR regions is one of the main strategies used to enhance the power conversion efficiency (PCE) of photovoltaic devices.<sup>1</sup> In dye-sensitized solar cells (DSSCs),<sup>2</sup> visible light is absorbed

by a suitable dye sensitizer adsorbed onto a thin film of a wide band-gap semiconductor, such as TiO<sub>2</sub>. Currently, the best-performing DSSCs are built using metal-free organic dyes, which allowed them to reach record PCE values above 15%.<sup>3</sup>

Several approaches have been tested to increase the LHE of DSSCs built with organic dyes, such as the use of panchromatic sensitizers<sup>4</sup> or the application of co-sensitization strategies.<sup>5</sup> However, the design of organic compounds exhibiting panchromatic absorption is far from trivial and their preparation is often lengthy and complicated; on the other hand, co-sensitization usually involves a tedious optimization process to determine the best experimental staining conditions.

For these reasons, in the last two decades,<sup>6</sup> another concept was explored to broaden the absorption profiles of dyes, exploiting the so-called Förster resonance energy transfer (FRET),<sup>7</sup> a mechanism by which energy can be transferred non-radiatively from an excited donor molecule to an acceptor one separated by a short enough distance. If the donor and acceptor have distinct light absorption profiles, the latter will be excited by photons to which it should normally be insensitive, significantly expanding its light harvesting ability. Traditionally, in DSSCs, FRET has been obtained by introducing energy-relay dyes (ERDs) in the liquid or solid electrolyte<sup>8–10</sup> or by co-adsorbing sensitizers and ERDs on the semiconductor surface.<sup>5,11–14</sup> However, considering that the FRET efficiency decreases steeply with the distance,<sup>6</sup> the use of molecular dyads, in which the sensitizer is bound to a suitable antenna, appears to be a promising alternative. Based on the early works by Amadelli *et al.*<sup>15</sup> and Siegers *et al.*<sup>16</sup> on Ru-based sensitizers, such an approach has been mostly applied to assemblies containing porphyrin, phthalocyanine and BODIPY units.<sup>8,17–19</sup> Conversely, the use of dyads featuring exclusively metal-free organic dyes has been less explored and was often limited to relatively small structures with simple push–pull architectures.<sup>20,21</sup>

Inspired by these reports, we reasoned that a possible advancement could be obtained by combining a D–A–π–A sensitizer, having strong absorption in the region of maximum

<sup>a</sup> CNR-ICCOM, Via Madonna del Piano 10, 50019 Sesto Fiorentino, Italy.

E-mail: [daniele.franchi@cnr.it](mailto:daniele.franchi@cnr.it), [alessio.dessi@cnr.it](mailto:alessio.dessi@cnr.it)

<sup>b</sup> Department of Chemistry “U. Schiff”, University of Florence,  
Via della Lastruccia 13, 50019 Sesto Fiorentino, Italy

<sup>c</sup> Department of Biotechnology, Chemistry and Pharmacy, R<sup>2</sup>ES Lab,  
University of Siena, Via A. Moro 2, 53100 Siena, Italy

<sup>d</sup> CSGI, Consorzio per lo Sviluppo dei Sistemi a Grande Interfase,  
Via della Lastruccia 3, 50019 Sesto Fiorentino, Italy

<sup>e</sup> Department of Chemical Sciences, University of Padua, Via F. Marzolo 1,  
35131 Padua, Italy

<sup>f</sup> CNR-ICMATE, c/o Department of Chemical Sciences, University of Padua,  
Via F. Marzolo 1, 35131 Padua, Italy

<sup>g</sup> Department of Chemical Sciences and Materials Technologies (DSCTM),  
National Research Council, P.le A. Moro 7, 00185 Rome, Italy

<sup>†</sup> Electronic supplementary information (ESI) available: Full computational details; full synthetic procedures; copies of the <sup>1</sup>H-NMR, <sup>13</sup>C-NMR and HRMS spectra of compounds **Ant-1**, **EE24** and **DYAD2**; details of spectroscopic, electrochemical and photovoltaic characterization experiments. See DOI: <https://doi.org/10.1039/d5cc02692j>

<sup>‡</sup> These authors contributed equally to this work.

<sup>§</sup> Current address: Department of Biological, Chemical and Pharmaceutical Sciences and Technologies, University of Palermo, Viale delle Scienze, Build. 16, 90128 Palermo, Italy.



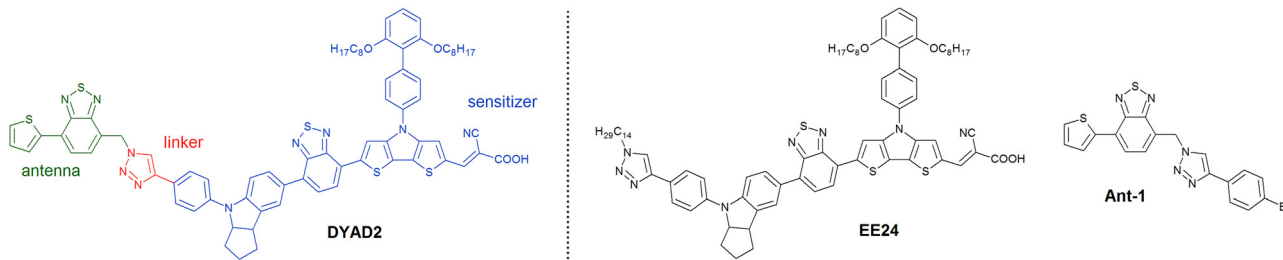


Fig. 1 Structures of the molecular dyad **DYAD2** and the model compounds **EE24** and **Ant-1**.

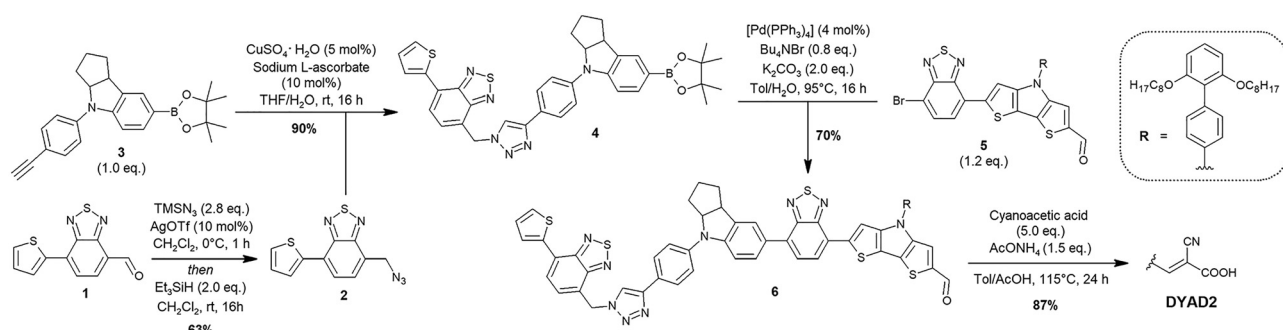
sunlight intensity (500–600 nm), with a bespoke antenna that can harvest higher energy photons and provide efficient FRET to the sensitizer, thanks to an optimal overlap between the respective absorption and emission spectra,<sup>6</sup> as suggested by previous computational studies on highly conjugated dyes.<sup>22</sup> Ideally, we aimed to combine the antenna and sensitizer units using a simple and robust methodology, allowing the orthogonal connection of differently functionalized fragments under mild conditions.

The designed dyad is shown in Fig. 1 (**DYAD2**). The sensitizer features a central benzothiadiazole–dithienopyrrole (BTD–DTP) chromophore, which was chosen for its strong light absorption ability in the visible region above 500 nm.<sup>23,24</sup> To further promote visible absorption, the sensitizer was endowed with a strong indoline donor group, whose nitrogen atom could also serve as a docking site for the antenna. The DTP unit was decorated with a bulky diphenyl fragment bearing long alkoxy chains to hinder charge recombination and dye aggregation phenomena.<sup>24</sup> Finally, the antenna was prepared using a thiophene–BTD fragment, which was selected based on previous studies on a similar ERD,<sup>25</sup> exhibiting a high fluorescence quantum yield and an emission spectrum that potentially matched very well with dye absorption. To connect the two dyad subunits, we set to apply the classic Cu-promoted azide–alkyne cycloaddition (CuAAC),<sup>26</sup> as already reported for other FRET ensembles.<sup>27</sup> Besides **DYAD2**, we also designed and prepared the detached model dye **EE24** and antenna **Ant-1**, which were used as reference compounds throughout the following studies.

Before synthesis, the electronic and photophysical properties of the compounds were assessed by density functional

theory (DFT) and time-dependent DFT (TDDFT) computational methods (see the ESI† for details). As expected, the energy separation between frontier molecular orbitals (FMOs) was much larger for **Ant-1** compared to **EE24**: as a result, the FMOs of **DYAD2** essentially resembled those of the isolated dye, with the HOMO mostly located on the indoline donor and the LUMO on the cyanoacrylic acceptor (Fig. S3 and S4, ESI†); LUMO+1, on the other hand, corresponded to the LUMO of **Ant-1**, thus being confined on the thiophene–BTD fragment. TDDFT calculations indicated that the main visible absorption of **DYAD2** and **EE24** was in the 540–570 nm range (Table S1, ESI†), which was completely decoupled from that of the antenna (ca. 400 nm); the latter, however, had a computed emission at ca. 500 nm (Table S2, ESI†), confirming the possibility of extended overlap with the sensitizer absorption and thus efficient FRET between the two dyad subunits.

The synthetic route used to prepare the dyad is shown in Scheme 1, whereas details on the preparation of intermediates and compounds **EE24** and **Ant-1** are reported in the ESI.† First, aldehyde **1** was converted to azide **2** via a Lewis acid-mediated reaction with  $\text{TMN}_3$ , followed by *in situ* reduction of the incipient diazido intermediate. Then, the CuAAC reaction of azide **2** with functionalized alkyne **3** under classical conditions led to intermediate **4**, constituting the donor–antenna portion of the dyad, in good yield with perfect regioselectivity. The boronic ester moiety present on compound **4** was then exploited to carry out a Suzuki–Miyaura cross-coupling with bromide **5** bearing the main BTD–DTP chromophore, leading, after some optimization, to the formation of compound **6** in moderate yield. Finally, a Knoevenagel reaction under typical conditions allowed the conversion of the already-installed



Scheme 1 Synthetic route applied for the preparation of **DYAD2**.



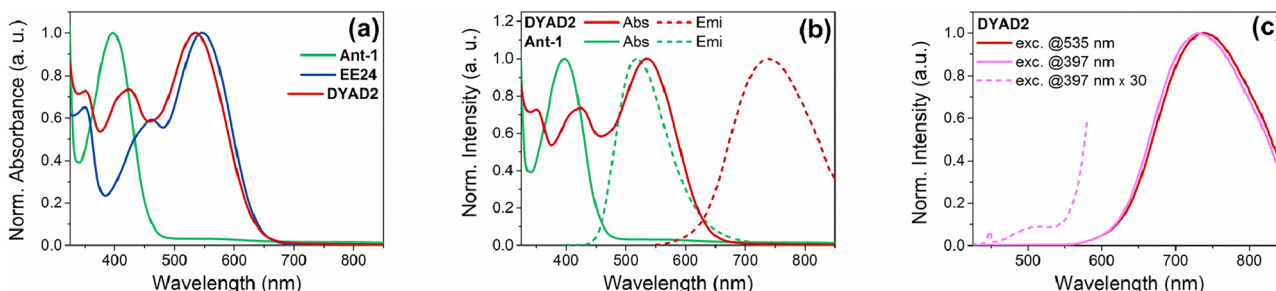


Fig. 2 (a) Normalized UV-Vis absorption spectra of **Ant-1**, **EE24** and **DYAD2** in THF solution; (b) normalized UV-Vis and fluorescence spectra of **Ant-1** and **DYAD2** in THF solution; and (c) normalized fluorescence spectra of **DYAD2** in THF solution at different excitation wavelengths.

aldehyde function in **6** into cyanoacrylic acid, thus completing the synthesis of **DYAD2**.

After their synthesis, the compounds were subjected to UV-Vis and fluorescence spectroscopy characterization in THF solution (Fig. S10, S11 and Table S3, ESI<sup>†</sup>). The absorption of **Ant-1** reached its maximum at *ca.* 400 nm, whereas the spectrum of **EE24** exhibited a  $\lambda_{\text{max}}$  at 546 nm and a minimum roughly matching **Ant-1** absorption (Fig. 2a). Both  $\lambda_{\text{max}}$  values were in good agreement with the calculations. **DYAD2** showed a higher molar absorptivity (Table S3, ESI<sup>†</sup>) and an enhanced light absorption ability in the 350–450 nm region compared to **EE24**, thanks to light harvesting by the antenna. Fig. 2a also shows that its normalized absorption profile above 500 nm was almost coincident with that of the reference dye. Upon adsorption on  $\text{TiO}_2$  (Fig. S13, ESI<sup>†</sup>), the spectra of **EE24** and **DYAD2** maintained similar shapes, albeit with slight shifts of the maxima. Compared to the solution, the increase of LHE in the violet-blue region for **DYAD2** was less notable, probably due to the underlying  $\text{TiO}_2$  absorption starting at 420 nm. Fig. 2b shows the comparison between the absorption spectra of **DYAD2** and **Ant-1** emissions in THF: as predicted by TDDFT calculations, an almost perfect overlap could be observed, confirming the possibility of efficient FRET. Upon irradiation of **DYAD2** at 397 and 535 nm (excitation of the antenna and the sensitizer units, respectively), almost identical fluorescence spectra were observed with  $\lambda_{\text{max}}$  at 729–737 nm (Fig. 2c) and a very small residual emission of the antenna around 500 nm (see the curve with 30× magnification), suggesting the occurrence of energy transfer between the two parts of the dyad. This was further supported by comparing the shapes of the excitation spectra of **EE24** and **DYAD2** showing fluorescence close to the emission maxima (Fig. S14, ESI<sup>†</sup>). Both spectra resembled the corresponding absorption profiles very closely: accordingly, for **DYAD2**, the emission intensity for excitation in the 350–450 nm range was clearly higher than that for **EE24**, indicating that, besides internal conversion from a higher excited state of the sensitizer, absorption by the antenna was also contributing to emission at longer wavelengths. Characterization of the sensitizers was completed by assessing their ground- and excited-state oxidation potentials (Fig. S15 and Table S3, ESI<sup>†</sup>), confirming that for both compounds regeneration using a typical DSSC electrolyte and electron injection into  $\text{TiO}_2$  were thermodynamically feasible.

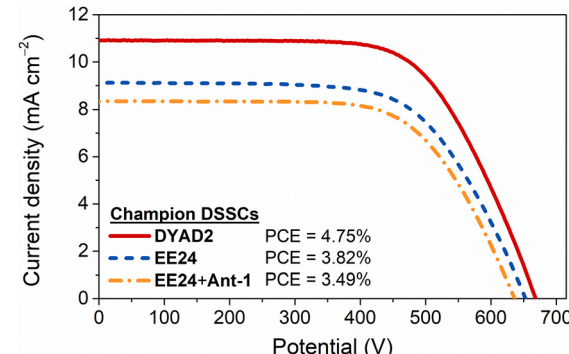


Fig. 3 *J/V* curves of the best DSSCs (area = 0.25 cm<sup>2</sup>) built with sensitizers **EE24** and **DYAD2**.

Based on the DFT and spectroscopic studies, we calculated the relevant FRET parameters (see the ESI<sup>†</sup> for details). The FRET radius ( $R_0$ ), defined as the distance at which the ET efficiency is 50%, was found to be 45.0 Å. Considering a computed antenna–sensitizer distance of 17.6 Å, we thus calculated an almost quantitative FRET efficiency ( $E_{\text{FRET}}$ ) above 99%. This parameter was also determined experimentally by measuring the fluorescence lifetime of the antenna alone (in **Ant-1**) and in the presence of the sensitizer (in **DYAD2**). From these data (Fig. S16 and Table S4, ESI<sup>†</sup>), we obtained an  $E_{\text{FRET}}$  value of 88%, which, albeit smaller than the computed one, still supported the occurrence of highly efficient energy transfer within the dyad (see the ESI<sup>†</sup> for discussion).

To conclude our study, we compared the performances of DSSCs built using **DYAD2**-sensitized  $\text{TiO}_2$  photoanodes with those of cells containing **EE24** (see the ESI<sup>†</sup>), with or without **Ant-1** added to a typical  $\text{I}^-/\text{I}_3^-$ -based electrolyte (Fig. 3). It should be noted that the cell fabrication procedure was not fully optimized, since our goal was to detect differences in device performances, rather than obtain high PCE values. As reported in Table S5 (ESI<sup>†</sup>), cells built with **DYAD2** performed better than those containing **EE24**, displaying an average PCE of 4.4% *vs.* 3.2% (+35%). Addition of 0.01 M **Ant-1** into the electrolyte, on the other hand, had little effect on the average PCE and even resulted in a worse champion cell (Fig. 3). The increase of PCE for **DYAD2** was mostly due to a higher photocurrent ( $J_{\text{sc}}$ ): accordingly, cells built with **DYAD2** showed



enhanced IPCE spectra compared to those containing **EE24** (Fig. S17, ESI†). The largest difference was observed at *ca.* 400 nm, in correspondence with the maximum absorption of the antenna (Fig. S18, ESI†), further supporting the hypothesis that improved device LHE could result from effective intramolecular energy transfer within the dyad, while intermolecular energy transfer did not occur efficiently under the conditions tested.

In summary, we reported the synthesis, characterization and application in DSSCs of a fully organic covalent dyad (**DYAD2**) based on a novel molecular design, which comprised a D-A- $\pi$ -A BTD-DTP dye attached to a BTD-based antenna, whose structure was tailored to maximize the overlap between the antenna emission spectrum and the dye absorption spectrum. The occurrence of FRET within the dyad was demonstrated using both stationary and time-resolved spectroscopy experiments. We measured an energy transfer efficiency of *ca.* 88% in solution, which, to the best of our knowledge, has not been reported previously for fully organic dyads used in DSSCs and is among the highest recorded values for such systems (see Table S6 for a comparison with literature data, ESI†). Preliminary experiments on DSSCs built with **DYAD2** showed better LHE compared to the reference dye **EE24** without the antenna unit, resulting in markedly higher average  $J_{sc}$  (+37%) and PCE (+35%) values, which was confirmed by the enhancement of the corresponding IPCE spectrum. Studies on the synthesis of further covalent dyads and optimization of DSSC performances are ongoing, and their results will be reported in due course.

A statement concerning individual authors' contributions is available in the ESI.†

This work was supported by the Research Fund for the Italian Electrical System through projects "CANVAS", PTR 2019-2021, type-A call, D. M. 182 of 5/8/2022 and "High-efficiency photovoltaics", PTR 2022-2024, D. M. 337 of 15/9/2022, and by CNR through projects "FOE2020 – Capitale naturale e risorse per il futuro dell'Italia" and "FOE2022 – FuturRaw". We thank Dr M. Di Donato (CNR-ICCOM), Prof. E. Collini and Dr I. Fortunati (Univ. of Padua) for helpful discussions, and Mr C. Bartoli (CNR-ICCOM) for technical assistance.

## Data availability

Data for this article are available at <https://zenodo.org> (<https://doi.org/10.5281/zenodo.15357783>).

## Conflicts of interest

The authors declare no competing financial interests.

## Notes and references

- G. Han, S. Zhang, P. P. Boix, L. H. Wong, L. Sun and S.-Y. Lien, *Prog. Mater. Sci.*, 2017, **87**, 246.
- A. Hagfeldt, G. Boschloo, L. Sun, L. Kloo and H. Pettersson, *Chem. Rev.*, 2010, **110**, 6595.
- Y. Ren, D. Zhang, J. Suo, Y. Cao, F. T. Eickemeyer, N. Vlachopoulos, S. M. Zakeeruddin, A. Hagfeldt and M. Grätzel, *Nature*, 2023, **613**, 60.
- J. Watson, T. J. Santaloci, H. Cheema, R. C. Fortenberry and J. H. Delcamp, *J. Phys. Chem. C*, 2020, **124**, 25211.
- J. M. Cole, G. Pepe, O. K. Al Bahri and C. B. Cooper, *Chem. Rev.*, 2019, **119**, 7279.
- J. I. Basham, G. K. Mor and C. A. Grimes, *ACS Nano*, 2010, **4**, 1253.
- T. Förster, *Discuss. Faraday Soc.*, 1959, **27**, 7.
- F. Odobel, Y. Pellegrin and J. Warnan, *Energy Environ. Sci.*, 2013, **6**, 2041, and references cited therein.
- M. M. Rahman, M. J. Ko and J.-J. Lee, *Nanoscale*, 2015, **7**, 3526.
- S. Seok, B. S. Goud, S. Gwak, R. K. Chitumalla, J. Lim, W. Lee, C. T. T. Thuy, S. Vuppala, J. Jang, G. Kooyada and J. H. Kim, *J. Mol. Struct.*, 2022, **1249**, 131576.
- M. Shrestha, L. Si, C.-W. Chang, H. He, A. Sykes, C.-Y. Lin and E. W.-G. Diau, *J. Phys. Chem. C*, 2012, **116**, 10451.
- E. L. Unger, S. J. Fretz, B. Lim, G. Y. Margulis, M. D. McGehee and T. D. P. Stack, *Phys. Chem. Chem. Phys.*, 2015, **17**, 6565.
- Y.-J. Lin, J.-W. Chen, P.-T. Hsiao, Y.-L. Tung, C.-C. Chang and C.-M. Chen, *J. Mater. Chem. A*, 2017, **5**, 9081.
- A. Pradhan, M. S. Kiran, G. Kapil, S. Hayase and S. S. Pandey, *Sol. Energy Mater. Sol. Cells*, 2019, **195**, 122.
- R. Amadelli, R. Argazzi, C. A. Bignozzi and F. Scandola, *J. Am. Chem. Soc.*, 1990, **112**, 7099.
- C. Siegers, J. Hohl-Ebinger, B. Zimmermann, U. Würfel, R. Mülhaupt, A. Hinsch and R. Haag, *Chem. Phys. Chem.*, 2007, **8**, 1548.
- H. Choi, N. Cho, S. Paek and J. Ko, *J. Phys. Chem. C*, 2014, **118**, 16319.
- S. Yamamoto, S. Mori, P. Wagner, A. J. Mozer and M. Kimura, *Isr. J. Chem.*, 2016, **56**, 175.
- L. Zhao, *R. Soc. Open Sci.*, 2018, **5**, 181218, and references cited therein.
- G. Marotta, M. A. Reddy, S. P. Singh, A. Islam, L. Han, F. De Angelis, M. Pastore and M. Chandrasekharan, *ACS Appl. Mater. Interfaces*, 2013, **5**, 9635.
- K. S. V. Gupta, J. Zhang, G. Marotta, M. A. Reddy, S. P. Singh, A. Islam, L. Han, F. De Angelis, M. Chandrasekharan and M. Pastore, *Dyes Pigm.*, 2015, **113**, 536.
- W.-L. Ding, Q.-S. Li and Z.-S. Li, *J. Mater. Chem. A*, 2015, **3**, 19948.
- Y. Xie, W. Wu, H. Zhu, J. Liu, W. Zhang, H. Tian and W.-H. Zhu, *Chem. Sci.*, 2016, **7**, 544.
- A. Densi, D. A. Chalkias, S. Bilancia, A. Sinicropi, M. Calamante, A. Mordini, A. Karavotti, E. Stathatos, L. Zani and G. Reginato, *Sustainable Energy Fuels*, 2021, **5**, 1171.
- J. H. Cheon, S. A. Kim, K.-S. Ahn, M.-S. Kang and J. H. Kim, *Electrochim. Acta*, 2012, **68**, 240.
- J. E. Hein and V. V. Fokin, *Chem. Soc. Rev.*, 2010, **39**, 1302.
- R. Schütz, S. Malhotra, I. Thomas, C. Strothkämper, A. Bartelt, K. Schwarburg, T. Hannappel, C. Fasting and R. Eichberger, *J. Phys. Chem. C*, 2014, **118**, 9336.

